

1 **Local translation provides the asymmetric distribution of CaMKII required for**  
2 **associative memory formation**

3

4 Abbreviated Title: Local translation builds the presynaptic proteome

5

6

7 Nannan Chen<sup>1</sup>, Yunpeng Zhang<sup>1</sup>, Mohamed Adel<sup>1</sup>, Elena A. Kuklin<sup>1</sup>, Martha L. Reed<sup>1</sup>, Jacob  
8 D. Mardovin<sup>1</sup>, Baskar Bakthavachalu<sup>3†</sup>, K. VijayRaghavan<sup>3</sup>, Mani Ramaswami<sup>2,3</sup> and Leslie  
9 C. Griffith<sup>1\*</sup>

10

11 <sup>1</sup>Department of Biology, Volen National Center for Complex Systems, Brandeis University,  
12 Waltham, MA 02454-9110, USA

13

14 <sup>2</sup>Trinity College Institute of Neuroscience, School of Genetics and Microbiology and School  
15 of Natural Sciences, Trinity College Dublin, Dublin-2, Ireland

16

17 <sup>3</sup>National Centre for Biological Sciences, Tata Institute of Fundamental Research  
18 Bellary Road, Bangalore 560065, India and School of Basic Science, Indian Institute of  
19 Technology Mandi, India.

20

21 † Current Address: Tata Institute for Genetics and Society-Centre at inStem, Bellary Road,  
22 Bangalore 560065, India, and School of Basic Science, Indian Institute of Technology  
23 Mandi, India.

24

25 \*Corresponding author:

26

27 Leslie C. Griffith

28 Dept. of Biology MS008

29 Brandeis University

30 415 South St.

31 Waltham, MA 02454-9110

32 Tel: 781 736 3125

33 FAX: 781 736 3107

34 Email: [griffith@brandeis.edu](mailto:griffith@brandeis.edu)

35

36 **SUMMARY**

37           How compartment-specific local proteomes are generated and maintained is  
38 inadequately understood, particularly in neurons, which display extreme asymmetries. Here we  
39 show that local enrichment of Ca<sup>2+</sup>/calmodulin-dependent protein kinase II (CaMKII) in axons  
40 of *Drosophila* mushroom body neurons is necessary for cellular plasticity and associative  
41 memory formation. Enrichment is achieved via enhanced axoplasmic translation of *CaMKII*  
42 mRNA, through a mechanism requiring the RNA-binding protein Mub and a 23-base Mub-  
43 recognition element in the *CaMKII* 3'UTR. Perturbation of either dramatically reduces axonal,  
44 but not somatic, CaMKII protein without altering the distribution or amount of mRNA *in vivo*  
45 and both are necessary and sufficient to enhance axonal translation of reporter  
46 mRNA. Together, these data identify elevated levels of translation of an evenly distributed  
47 mRNA as a novel strategy for generating subcellular biochemical asymmetries. They further  
48 demonstrate the importance of distributional asymmetry in the computational and biological  
49 functions of neurons.

50

51

52

53 **KEYWORDS:** RNA-binding protein; synaptic plasticity; axonal translation;  
54 Calcium/calmodulin-dependent protein kinase II; mushroom body; *Drosophila*

## 55 INTRODUCTION

56 CaMKII is crucial to behavioral plasticity across phyla [1-3]. The resting concentration  
57 of CaMKII is extraordinarily high, reaching 2% of total protein in the mammalian hippocampus  
58 [4], with most concentrated in synaptic regions. The 3'UTRs of both mammalian *CAMK2A*  
59 and *Drosophila CaMKII* contain regulatory information important for activity-dependent  
60 plasticity-related local translation in dendrites [5, 6] and presynaptic terminals respectively [7,  
61 8]. While this acute modulation of CaMKII translation by neural activity has been described in  
62 multiple species, the mechanisms establishing, and indeed the function of, the impressive basal  
63 synaptic enrichment of CaMKII are completely unknown in any species.

64

## 65 RESULTS

66

### 67 CaMKII is enriched in axons via an active process

68 To visualize the extent of synaptic enrichment in *Drosophila melanogaster*, we  
69 expressed soluble GFP, which distributes in the cell via diffusion, under control of *CaMKII-*  
70 *GAL4* (Figure S1A), a driver transgene in the *CaMKII* locus, and compared its distribution to  
71 that of endogenous CaMKII. We focused on the mushroom body (MB), which is composed of  
72 Kenyon cells (KCs) with distinct somatic, dendritic and axonal compartments [9] (Figure 1A)  
73 whose plasticity is central to memory formation in *Drosophila* [10]. Figures 1B-C show the  
74 axon/soma ratio for soluble GFP is significantly lower than that of CaMKII suggesting that an  
75 active process regulates localization of CaMKII protein. This MB neuropil enrichment occurs  
76 specifically in KC axons, and is not due to CaMKII from extrinsic neuronal processes in the  
77 neuropil, as it is seen when the endogenous *CaMKII* gene is tagged with EGFP via  
78 CRISPR/Cas9 [11] exclusively in MBs (Figures 1D-F and S1B-C). Population of the synaptic  
79 region by trapping or stabilization of CaMKII can also be ruled out, since an EYFP::CaMKII  
80 fusion protein [12] expressed under control of GAL4 expresses at equivalent levels in cell  
81 bodies and axons (Figures 1G-H). These data suggest that non-coding regions (UTRs) of the  
82 *CaMKII* mRNA may control presynaptic accumulation of CaMKII protein.

83

### 84 The *CaMKII* 3'UTR contains multiple independent regulatory *cis*-elements

85 To ask if the *CaMKII* 5' or 3' UTR could mediate synaptic enrichment of protein in  
86 adult brain we generated animals with a GAL4-driven mMaple3 [13] coding sequence followed  
87 by either the long or short form of the 3'UTR (1990 and 123 bp respectively, produced by  
88 alternative polyadenylation [8]), or preceded by the 5'UTR of CaMKII (Figure 2A). All  
89 transgenes, including the control, which has no *CaMKII* UTR sequences, contain an SV40

90 polyadenylation site. Expression of these transgenes in KCs resulted in similar mMaple3  
91 fluorescence in the somatic regions of all four lines (Figures S2A-B). Examination of the  
92 axonal processes of the MB, however, revealed a marked enrichment of mMaple3 protein in  
93 the MB lobes when the reporter was followed by the full 3'UTR (Figures 2B-C). Since  
94 mMaple3, like GFP, is a soluble cytosolic protein, somatically-synthesized protein can only  
95 reach axon terminals of the lobes by diffusion or transport. The ability of the long 3'UTR of  
96 CaMKII to concentrate mMaple3 at the synaptic terminal, without changing somatic protein  
97 levels, strongly suggests that the distal *CaMKII* 3'UTR is altering the location of protein  
98 synthesis.

99 Both the proximal and distal ends of the *CaMKII* 3'UTR are highly conserved in insects  
100 (<http://genome.ucsc.edu>), but only the function of the proximal and non-conserved middle  
101 regions have been previously studied due to incomplete annotation of the region leading to use  
102 of a truncated 3'UTR in previous studies [12]. The idea that 3'UTRs are modularized to execute  
103 multiple functions led us to explore the role of the conserved and unconserved pieces  
104 individually by making additional mMaple3 transgenes (Figure 2A) and examining their  
105 effects on protein and steady-state mRNA levels (Figures 2B-C). The proximal conserved  
106 region (fragment I) increased both mRNA and somatic mMaple3 compared to the SV40-only  
107 control (Figures 2C and S2A-C). However, these animals had about half the axonal mMaple3  
108 of the long 3'UTR transgene (Figure 2C), indicating that, while the distal part of fragment I  
109 likely contains an mRNA stability element, (see also Figure 4D), it lacks a translation enhancer.  
110 Consistent with this, the non-conserved (II) and distal conserved (III) fragments had mRNA  
111 levels comparable to control and short 3'UTR transgenes, and lower protein expression in both  
112 soma and lobe compared to the full 3'UTR.

113 Interestingly, while the absolute levels of mMaple3 protein driven by fragment III were  
114 lower than the no-UTR control (suggesting the presence of translational repressor elements,  
115 see Figures 2C and S2B) the ratio of axonal to somatic protein appeared to be higher than for  
116 other transgenes, providing a hint that this region might harbor regulatory information for  
117 axonal translation. Additionally, this region is highly conserved across insect species,  
118 motivating us to subdivide it further. Division allowed us to map translational repressors to the  
119 proximal (III-1) and distal (III-3) parts of fragment III and revealed a strong axonal translation  
120 enhancer in fragment III-2 (Figures 2B-C). mRNA levels for all three were equivalent to  
121 control (Figures 2C and S2C). Both lobe (Figure 2C) and soma (Figure S2B) mMaple levels  
122 with the 286bp III-2 fragment were equal to those produced by the full length 3'UTR,  
123 suggesting that it contains the *cis*-element which is the major driver of axonal accumulation of  
124 CaMKII (Figure 2E).

125

126 **The distal *CaMKII* 3'UTR drives axonal protein enrichment via a translational**  
127 **mechanism**

128 To determine if the enrichment of CaMKII protein was due to 3'UTR-dependent  
129 localization of mRNA or 3'UTR-dependent translation within the presynaptic compartment,  
130 we employed a second set of transgenes which contained, in addition to a myrGFP translation  
131 reporter, a 24-repeat MS2 string that allows detection of mRNA with transgenically-expressed  
132 MCP::RFP [14]. Figure 2D shows that there is no difference in the amount of axonal mRNA  
133 between transgenes containing short or full length 3'UTRs. This accumulation of MCP::RFP  
134 in axons was completely dependent on co-expression of an MS2 transgene (Figures S2E and  
135 S2G). As with the mMaple3 reporters, the presence of the distal 3'UTR significantly increased  
136 axonal myrGFP protein accumulation (Figures S2D and S2F), consistent with a role in  
137 translational regulation rather than mRNA localization. To ask if MB axonal processes have  
138 the machinery for local translation, we expressed a GFP-tagged ribosomal subunit that has been  
139 shown to assemble with endogenous ribosomes [15] and found that it localizes to axons (Figure  
140 S2H), consistent with the presence of ribosomes. Taken together, these results support the idea  
141 that the distal part of the *CaMKII* 3'UTR specifies presynaptic accumulation of protein via a  
142 translational mechanism.

143

144 **RNA-binding protein Mub directs axonal protein accumulation**

145 *Trans*-acting factors, including RNA-binding proteins (RBPs), function as the  
146 executors of the programs encoded in *cis*-elements [16]. To identify RBPs that might act on  
147 the *CaMKII* 3'UTR, we performed an *in silico* screen with RBPmap [17] and found that there  
148 were few RBPs predicted to bind only to the distal regions (Figures S3A-B). We assayed the  
149 function of these candidates by examining the effect of RNAis on reporter protein levels in  
150 animals expressing the *mMaple3-III-2* transgene. Only knock-down of *mushroom body*  
151 *expressed (mub)* [18], the widely-expressed single ortholog of the mammalian poly-C-binding-  
152 protein family, significantly decreased axonal mMaple3 protein expression (Figures 3A-B).  
153 Knockdown of RBPs that more generally bind the distal 3'UTR identified several candidate  
154 repressors (Figure S3C-D).

155 While the RNAi results were consistent with Mub directly regulating reporter  
156 accumulation via the *CaMKII* 3'UTR, it was also possible that the decrease in mMaple3 protein  
157 was due to a more general or indirect function of Mub. To determine if the effect of Mub  
158 knockdown was direct, we mutated predicted Mub-binding sites within the 3'UTR and asked  
159 if that affected mMaple3 protein levels in axons. We used a transgene that contained both

160 fragments III-2 and -3 since Mub has two binding sites in fragment III, one of which spans the  
161 III-2/3 junction. Both A->T point mutations in the two sites, or deletion of the 23bp containing  
162 the sites, decreased mMaple protein expression in axons (Figures 3C-D). Notably, the 23bp  
163 element alone was sufficient to raise expression over the level of the WT fragment (Figures  
164 3C-D). Importantly, somatic mMaple3 levels were not significantly changed by loss of Mub  
165 sites (Figure 3D). We speculate that this, as well as the high activity of the isolated 23bp  
166 fragment, is due to the presence of repressor sequences in region III-3 that normally act to  
167 block translational stimulation by Mub in the cell body.

168 While early studies [18] and our *Mub-GAL4* line (Figure S1D) suggested that the *mub*  
169 gene is transcribed in MB, it was important to determine where the Mub protein was localized  
170 within the MB. We used CRISPR/Cas9 [11] to fuse EGFP in-frame to the N-terminal of the  
171 Mub coding region. Consistent with *Mub-GAL4*'s expression pattern, EGFP::Mub protein was  
172 widely-expressed, and almost exclusively somatic in the adult brain. The one remarkable  
173 exception was the MB, where EGFP::Mub can be seen in axonal processes (Figure 3E). These  
174 data suggest that Mub has a unique role in CaMKII axonal translation in KCs (Figure 3F).

175

### 176 **Mub sites in the *CaMKII* 3'UTR mediate formation of the basal proteome and support** 177 **associative memory formation**

178 To explore the function of the distal 3'UTR in the context of the endogenous *CaMKII*  
179 locus, we used CRISPR/Cas9 [11] to replace the entire 3'UTR with an attP-flanked 3XP3-RFP  
180 recombination cassette, creating *CaMKII<sup>U<sup>Del</sup></sup>* (Figure 4A). We then replaced 3XP3-RFP using  
181 attB-flanked 3'UTR sequences to engineer full, short and Mub-site mutant 3'UTR lines  
182 (*CaMKII<sup>U<sup>Long</sup></sup>*, *CaMKII<sup>U<sup>Short</sup></sup>* and *CaMKII<sup>ΔMubS</sup>*) (Figure 4A). Both *CaMKII<sup>U<sup>Short</sup></sup>* and  
183 *CaMKII<sup>ΔMubS</sup>* had drastically decreased axonal (Figures 4B-C) and total head CaMKII protein  
184 (Figures S4A-B) compared to *CaMKII<sup>U<sup>Long</sup></sup>*. Levels of mRNA for *CaMKII<sup>U<sup>Long</sup></sup>* and  
185 *CaMKII<sup>ΔMubS</sup>* were not different (Figure 4D). *CaMKII<sup>U<sup>Short</sup></sup>* mRNA was ~10% lower, likely due  
186 to loss of a stability element (see Figure 2E), but this decrease is not enough to account for the  
187 ~75% decrease in protein. These data suggest that loss of the 23bp Mub site renders animals  
188 incapable of generating high basal axonal CaMKII protein despite the fact that total mRNA  
189 levels are normal (Figure 4D).

190 We next asked if CaMKII accumulation in axons was needed for MB plasticity by  
191 assaying short-term associative memory in 3'UTR-mutant lines. Loss of the distal 3'UTR  
192 significantly impaired both appetitive (Figure 4E) and aversive (Figure 4F) associative memory  
193 formation. This defect mapped to the Mub-binding element since animals lacking only the  
194 23bp site were almost totally unable to learn (Figures 4E-F). To determine if this plasticity



195 defect was a result of loss of axonal CaMKII specifically in KCs, we utilized a conditional  
196 allele, *CaMKII<sup>FRT-3'UTR-FRT</sup>* (Figure 4A) and removed the 3'UTR of the gene exclusively in KCs  
197 by expression of FLP recombinase. These animals, which have normal synaptic CaMKII in all  
198 cells except for KCs (Figures 4G-H and S4G), showed significant decreases in aversive  
199 associative memory formation (Figure 4I). Shock and odor detection were similar in these flies  
200 (Figures S4C-F and S4H-I).

201 A critical early event of associative memory formation in the  $\alpha'$  lobe of MB is  
202 potentiation of odor responses, postulated to be a memory trace or engram [19]. To determine  
203 if the basal CaMKII proteome was required for this cellular process, we utilized an *ex vivo*  
204 assay for pairing-dependent plasticity (PDP), a paradigm similar to long-term enhancement [20,  
205 21] in which stimulation of the antennal lobe olfactory inputs (the conditioned stimulus) is  
206 temporally paired with dopamine application (the unconditioned stimulus). Potentiation of the  
207 response to antennal lobe stimulation in the  $\alpha'3$  compartment was defective in both  
208 *CaMKII<sup>UShort</sup>* and *CaMKII <sup>$\Delta$ MubS</sup>* (Figure 4J). Importantly, the initial response of KCs to  
209 acetylcholine, the transmitter used by olfactory inputs to the MB, was not altered by UTR  
210 mutations (Figure S4J-S4M). These results demonstrate that the enrichment of CaMKII in the  
211 presynaptic proteome by a Mub-dependent mechanism is required for the plastic changes in  
212 odor responses that are a signature of associative memory formation (Figure 4K). This  
213 underscores the critical role of high levels of axonal CaMKII in the computational processes  
214 carried out in this compartment.

215

## 216 **DISCUSSION**

217

218 Local protein synthesis at synapses has been studied extensively in the context of  
219 specialized processes like activity-dependent plasticity and axon guidance [22]. Recent theory  
220 and experimental work [23, 24], however, suggests that local translation occurs much more  
221 generally and may be used to establish differential proteomes in functionally-specialized  
222 subcellular regions. In this study we resolve two long-standing questions about CaMKII: how  
223 and why it achieves extraordinary levels in axons. We demonstrate that resting adult levels of  
224 CaMKII protein are translationally accrued, and that the high levels in this compartment form  
225 a computational scaffold critical for formation of associative memory and the cellular memory  
226 trace. While previous studies using mutants and RNAi have shown a role for CaMKII in  
227 plasticity, our manipulations of the 3'UTR, which do not affect somatic kinase levels, establish  
228 the necessity of synaptic enrichment. This enrichment requires *cis*-elements present only in the

229 long form of the 3'UTR and Mub, the *Drosophila* poly-C-binding-protein homolog  
230 demonstrating a new, activity-independent function for the *CaMKII* 3'UTR.

231 Activity-dependent translation [5, 7, 12, 25, 26] and differential polyadenylation [24,  
232 26] are ancient conserved features of CaMKII mRNAs. For mammalian *CAMK2A*, early work  
233 in which the 3'UTR was deleted demonstrated its requirement for mRNA stability and  
234 dendritic localization, and also for protein accumulation and activity-dependent synthesis [6].  
235 A handful of studies attempted to identify *cis*-elements regulating dendritic *CAMK2A* mRNA  
236 localization and transport [27-29], but there is as yet no information on 3'UTR *cis*-elements  
237 controlling translation, though *in silico* prediction suggests that the *CAMK2A* 3'UTR may have  
238 polyC-binding protein motifs.

239 At the *Drosophila* larval neuromuscular junction, we and others have shown that the  
240 *CaMKII* 3'UTR controls activity-dependent synthesis of CaMKII [7, 12, 26, 30]. The fact that  
241 the rodent *CAMK2A* 3'UTR can support activity-dependent protein synthesis in the fly [12]  
242 suggests that there will be shared mechanisms for this aspect of CaMKII regulation. But while  
243 there are many similarities between mammals and flies, there are also differences. In  
244 *Drosophila*, the 3'UTR appears to have little effect on mRNA localization, and only a small  
245 effect on stability that is ascribable to a proximal *cis*-element. How *CaMKII* mRNA reaches  
246 synapses in *Drosophila* is yet to be determined, but the differences in localization mechanism  
247 may reflect the ca. 100-fold difference in distances that mRNAs need to travel to reach  
248 synapses.

249 The ability of Mub, which is present at low levels in MB axons and at high levels in  
250 MB and other cell bodies, to specifically regulate axonal accumulation of CaMKII protein  
251 without affecting somatic protein levels suggests several models. One possibility is that MB  
252 axons have either compartment-specific translational machinery or a distinct set of auxiliary  
253 proteins that allow Mub to regulate axonal ribosomes [31, 32]. The presence of Mub protein in  
254 MB axons, but not in other neuropils, may indicate the existence of unique translational  
255 complexes in that compartment. Another possibility is that Mub is a general translation  
256 enhancer, but MB soma contain repressor proteins that locally inhibit its actions. This would  
257 be consistent with our finding that there are *cis* elements that appear to act as general repressors  
258 in the *CaMKII* 3'UTR. While these ideas remain speculative, the robust interaction of Mub  
259 with *CaMKII* provides an opportunity to deepen our understanding of how local protein  
260 synthesis can shape neuronal function and build the synaptic proteome.

261

262 **ACKNOWLEDGEMENTS**

263



264 We thank Ed Dougherty in the Brandeis Imaging Facility for assistance. Stocks obtained from  
265 the Bloomington Drosophila Stock Center (NIH P40 OD018537) were used in this study. This  
266 work was supported by NIH R37 NS112810 (to LCG), NIH R01 DA043195 (to LCG), a  
267 Science Foundation Ireland Investigator Programme Grant and Wellcome Trust-HRB-SFI  
268 Grants (to MR).

269

## 270 **AUTHOR CONTRIBUTIONS**

271

272 LCG and NC conceived the study and designed the experiments. NC, YZ and BB constructed  
273 fly lines. NC did all immunohistochemical analysis and qPCR. EAK did immunoblotting and  
274 analysis. NC, JDM and MLR did behavioral experiments. MA did electrophysiological  
275 experiments. All authors assisted with data analysis and interpretation. NC and LCG wrote the  
276 manuscript with input from all the authors.

277

## 278 **DECLARATION OF INTERESTS**

279

280 The authors declare no competing interests.

281

282

283 **Figure 1. CaMKII is enriched in presynaptic regions relative to cell bodies by an active**  
284 **process**

285 All transgenes were expressed with *VT030559-Gal4*, which is referred to in text/figures as  
286 “*MB-Gal4*” (A) Schematic diagram of mushroom body (MB) Kenyon cells. Dendritic  
287 processes, which receive inputs from the olfactory system, arborize adjacent to the somata,  
288 forming the “calyx”. Axonal processes extend ventrally to form the MB “lobes”.

289 (B) Representative images of adult brain somatic (top) and MB axon (bottom) regions of  
290 animals expressing soluble GFP under control of *CaMKII-GAL4* visualized with GFP and anti-  
291 CaMKII.

292 (C) Quantification of MB axon/soma ratio for CaMKII and soluble GFP. Data are mean  $\pm$  SEM  
293 analyzed by Student’s t-test. Gray dots show individual values. N = 22 for each group. \*\*\*  
294 indicates  $p < 0.001$ .

295 (D) Schematic of *Frt-stop-Frt-EGFP-CaMKII* allele and recombination strategy. To construct  
296 a conditional EGFP::CaMKII fusion allele, we first replaced exons 1-8 of *CaMKII* with an attP  
297 flanked *3P3>RFP* cassette to make the *CaMKII<sup>Coding-3P3-RFP</sup>* fly line. The RFP marker was then  
298 replaced by recombination of an attB-flanked *Frt-stop-Frt-EGFP* fused to the first eight exons  
299 of *CaMKII* to make the *Frt-stop-Frt-EGFP::CaMKII* fly strain. *Frt-stop-Frt* can be flipped out  
300 by cell-specific expression of Flp recombinase, allowing visualization of endogenous *CaMKII*  
301 protein levels.

302 (E) Representative images of *MB>Flp* activation of EGFP::CaMKII protein expression in  
303 axons (left) and somatodendritic regions (right) stained with DAPI and anti-Brp.

304 (F) Quantification of axon/soma ratio for EGFP::CaMKII. Data are mean  $\pm$  SEM. Gray dots  
305 show individual values. N = 10.

306 (G) Representative images of *MB-GAL4*-driven EYFP::CaMKII transgene lacking any  
307 *CaMKII* UTR. Axonal region (upper) and somatic region (lower) are shown.

308 (H) Ratio of axon/soma EYFP was ca. 1, indicating no enrichment in axons. Gray dots show  
309 individual values. N = 16.

310 Scale bars = 20  $\mu$ m for each panel. See also Figure S1.

311

312 **Figure 2. The distal *CaMKII* 3'UTR functions as the *cis*-element for axonal protein**  
313 **localization**

314 (A) Reporter transgenes used to screen for *cis*-elements. All transgenes were expressed with  
315 *VT030559-Gal4*, which is referred to in text/figures as “MB-Gal4”

316 (B) Representative images of mMaple3 protein in axons of *MB>mMaple3* animals. Scale bars  
317 = 20  $\mu$ m. Dashed white lines indicate MB axons.

318 (C) Left, mMaple3 protein levels in axons. N = 14-18. Right, qPCR of mRNA from adult *MB>*  
319 *mMaple3* heads using primers for *mMaple3*. N = 9-12. Red bars indicate significant increase  
320 relative to control, blue indicates decrease.

321 (D) Schematic of protein/RNA reporters (top), and representative images of axonal MCP::RFP  
322 (bottom). Long and short UTR mRNAs localized to neuropil equivalently. N = 12-14.

323 (E) Cartoon of *cis*-regulatory elements identified in this study. The long 3'UTR and fragment  
324 I both have higher levels of mRNA suggesting the presence of a stability element between the  
325 end of the short 3'UTR and the end of fragment I. The translational enhancer localizes to the  
326 III-2 region, while translational repressors localize to III-1 and III-3.

327 Data are shown as mean  $\pm$  SEM, analyzed by Student's t-test or one-way ANOVA with  
328 Bonferroni post-hoc test as appropriate. Gray dots show individual values. Statistical  
329 differences are indicated by letters in panel C, with genotypes that are not significantly different  
330 having the same letter. n.s. indicates no significant difference in panel D. See also Figure S2.

331

332 **Figure 3. Mub is the *trans*-factor specifying CaMKII axonal enrichment**

333 All transgenes were expressed with *VT030559-Gal4*, which is referred to in text/figures as  
334 “MB-Gal4”. (A) Representative single confocal sections of *MB>mMaple3-III-2* protein  
335 expression  $\pm$  RNAi knock-down of RBPs predicted to bind to distal regions.

336 (B) Quantification of MB axonal mMaple3 protein in *MB>mMaple3-III-2*  $\pm$  RNAi brains. N =  
337 18-26.

338 (C) Left, schematic of transgenes with Mub site manipulations. Right, representative pictures  
339 of mMaple3 in *MB>mMaple3-MubS* axons.

340 (D) Quantification of axonal and somatic mMaple3 protein levels from Mub site mutant  
341 transgenes. Loss of Mub-binding reduced mMaple3 in axons, while leaving somatic levels  
342 unchanged. The isolated 23bp Mub binding site elevated axonal protein over the level of  
343 control, and slightly elevated somatic levels, consistent the presence of repressor elements in  
344 the control UTR fragment. N = 12-18.

345 (E) Diagram of CRISPR-engineered *EGFP::Mub* allele. Images show EGFP for whole brain,  
346 MB axons and soma.

347 (F) Cartoon summary of Mub manipulations. Red X indicates no expression of Mub.

348 For all panels: Scale bars = 20  $\mu$ m. Dashed white lines indicate the MB axons. Data are mean  
349  $\pm$  SEM and quantified by one-way ANOVA with Bonferroni post-hoc test. Gray dots show  
350 individual values. Statistical differences are indicated by letters; groups that are not  
351 significantly different have the same letter. See also Figure S3.

352

353 **Figure 4. Loss of Mub-binding sites in the *CaMKII* 3'UTR impairs plasticity and memory**  
354 **formation**

355 All transgenes were expressed with *VT030559-Gal4*, which is referred to in text/figures as  
356 “MB-Gal4” (A) Diagram of CRISPR-engineered *CaMKII* alleles. *CaMKII<sup>Udel</sup>* has the entire  
357 3'UTR replaced by a recombination site-flanked 3P3>RFP transgene; other lines were  
358 generated from this by recombination. Endogenous *CaMKII* exons are indicated in gray, and  
359 replaced regions in color.

360 (B) Representative images of MB axon CaMKII protein levels in *CaMKII<sup>ULong</sup>*, *CaMKII<sup>UShort</sup>*  
361 and *CaMKII<sup>ΔMubS</sup>*. Dotted white lines indicate axonal region. Scale bars = 20  $\mu$ m.

362 (C) Anti-CaMKII staining in MB axons is reduced in *CaMKII<sup>UShort</sup>* and *CaMKII<sup>ΔMubS</sup>*. N = 18-  
363 25.

364 (D) *CaMKII* mRNA levels measured by qPCR of total head mRNA are slight lower in  
365 *CaMKII<sup>UShort</sup>*, but not affected by loss of Mub sites. N = 9 for each group.

366 (E) Appetitive short-term memory is disrupted in *CaMKII<sup>UShort</sup>* and *CaMKII<sup>ΔMubS</sup>*. N = 8-16.

367 (F) Aversive short-term memory is disrupted in *CaMKII<sup>UShort</sup>* and *CaMKII<sup>ΔMubS</sup>*. N = 13-21.

368 (G) Representative pictures of MB-specific deletion of the 3'UTR. Dotted white line indicates  
369 MB axons. Scale bars = 20 μm.

370 (H) CaMKII protein is reduced exclusively in MB axons when the 3'UTR is specifically  
371 knocked out in MB. N = 18 per group.

372 (I) Aversive short-term memory is disrupted when the 3'UTR is deleted specifically in MB. N  
373 = 14-17.

374 (J) Left, diagram of PDP paradigm. Antennae lobe stimulation trains (ES, white bars) and  
375 dopamine perfusion (DA, solid gray bar) are paired for 1 min. Right, Post-pairing calcium  
376 response increased significantly in *CaMKII<sup>ULong</sup>*, but not in *CaMKII<sup>UShort</sup>* or *CaMKII<sup>ΔMubS</sup>*.  
377 Circles and squares show individual values. Data were analyzed by paired-T-test, n.s. indicates  
378 no significant difference, \*\* indicates p<0.01.

379 (K) Model. Potentiation of calcium responses by association requires high levels of synaptic  
380 CaMKII. When Mub sites are lost, presynaptic CaMKII protein is reduced, and MB plasticity  
381 and memory formation are blocked.

382 Except for panel J, data are mean ± SEM analyzed by one-way ANOVA with Bonferroni post-  
383 hoc test. Gray dots show individual data points. Statistical differences are indicated by letters;  
384 groups that are not significantly different have the same letter. See also Figure S4.

385

386

387 **REFERENCES**

388

389 1. Griffith, L.C., Verselis, L.M., Aitken, K.M., Kyriacou, C.P., and Greenspan, R.J. (1993).  
390 Inhibition of calcium/calmodulin-dependent protein kinase in *Drosophila* disrupts  
391 behavioral plasticity. *Neuron* 10, 501-509.

392 2. Silva, A.J., Paylor, R., Wehner, J.M., and Tonegawa, S. (1992). Impaired spatial  
393 learning in alpha-calcium-calmodulin kinase II mutant mice [see comments]. *Science*  
394 257, 206-211.

395 3. Bayer, K.U., and Schulman, H. (2019). CaM Kinase: Still Inspiring at 40. *Neuron* 103,  
396 380-394.

397 4. Erondy, N.E., and Kennedy, M.B. (1985). Regional distribution of type II  
398 Ca<sup>2+</sup>/calmodulin-dependent protein kinase in rat brain. *J Neurosci* 5, 3270-3277.

399 5. Aakalu, G., Smith, W.B., Nguyen, N., Jiang, C., and Schuman, E.M. (2001). Dynamic  
400 visualization of local protein synthesis in hippocampal neurons. *Neuron* 30, 489-502.

401 6. Miller, S., Yasuda, M., Coats, J.K., Jones, Y., Martone, M.E., and Mayford, M. (2002).  
402 Disruption of dendritic translation of CaMKIIalpha impairs stabilization of synaptic  
403 plasticity and memory consolidation. *Neuron* 36, 507-519.

404 7. Nesler, K.R., Starke, E.L., Boin, N.G., Ritz, M., and Barbee, S.A. (2016). Presynaptic  
405 CamKII regulates activity-dependent axon terminal growth. *Molecular and cellular*  
406 *neurosciences* 76, 33-41.

407 8. Kuklin, E.A., Alkins, S., Bakthavachalu, B., Genco, M.C., Sudhakaran, I., Raghavan,  
408 K.V., Ramaswami, M., and Griffith, L.C. (2017). The Long 3'UTR mRNA of CaMKII  
409 Is Essential for Translation-Dependent Plasticity of Spontaneous Release in *Drosophila*  
410 *melanogaster*. *J Neurosci* 37, 10554-10566.

411 9. Rolls, M.M., Satoh, D., Clyne, P.J., Henner, A.L., Uemura, T., and Doe, C.Q. (2007).  
412 Polarity and intracellular compartmentalization of *Drosophila* neurons. *Neural*  
413 *development* 2, 7.

414 10. Boto, T., Stahl, A., and Tomchik, S.M. (2020). Cellular and circuit mechanisms of  
415 olfactory associative learning in *Drosophila*. *J Neurogenet* 34, 36-46.

416 11. Bier, E., Harrison, M.M., O'Connor-Giles, K.M., and Wildonger, J. (2018). Advances  
417 in Engineering the Fly Genome with the CRISPR-Cas System. *Genetics* 208, 1-18.

418 12. Ashraf, S.I., McLoon, A.L., Sclarsic, S.M., and Kunes, S. (2006). Synaptic protein  
419 synthesis associated with memory is regulated by the RISC pathway in *Drosophila*.  
420 *Cell* 124, 191-205.



- 421 13. Wang, S., Moffitt, J.R., Dempsey, G.T., Xie, X.S., and Zhuang, X. (2014).  
422 Characterization and development of photoactivatable fluorescent proteins for single-  
423 molecule-based superresolution imaging. *Proc Natl Acad Sci U S A* *111*, 8452-8457.
- 424 14. Grunwald, D., and Singer, R.H. (2010). In vivo imaging of labelled endogenous beta-  
425 actin mRNA during nucleocytoplasmic transport. *Nature* *467*, 604-607.
- 426 15. Thomas, A., Lee, P.J., Dalton, J.E., Nomie, K.J., Stoica, L., Costa-Mattioli, M., Chang,  
427 P., Nuzhdin, S., Arbeitman, M.N., and Dierick, H.A. (2012). A versatile method for cell-  
428 specific profiling of translated mRNAs in *Drosophila*. *PLoS ONE* *7*, e40276.
- 429 16. Bae, B., and Miura, P. (2020). Emerging Roles for 3' UTRs in Neurons. *Int J Mol Sci*  
430 *21*.
- 431 17. Paz, I., Kosti, I., Ares, M., Jr., Cline, M., and Mandel-Gutfreund, Y. (2014). RBPmap:  
432 a web server for mapping binding sites of RNA-binding proteins. *Nucleic Acids Res*  
433 *42*, W361-367.
- 434 18. Grams, R., and Korge, G. (1998). The mub gene encodes a protein containing three KH  
435 domains and is expressed in the mushroom bodies of *Drosophila melanogaster*. *Gene*  
436 *215*, 191-201.
- 437 19. Davis, R.L. (2011). Traces of *Drosophila* memory. *Neuron* *70*, 8-19.
- 438 20. Ueno, K., Naganos, S., Hirano, Y., Horiuchi, J., and Saitoe, M. (2013). Long-term  
439 enhancement of synaptic transmission between antennal lobe and mushroom body in  
440 cultured *Drosophila* brain. *J Physiol* *591*, 287-302.
- 441 21. Adel, M., and Griffith, L.C. (2021). Associative memory in a dish. In preparation.
- 442 22. Holt, C.E., Martin, K.C., and Schuman, E.M. (2019). Local translation in neurons:  
443 visualization and function. *Nat Struct Mol Biol* *26*, 557-566.
- 444 23. Fonkeu, Y., Kraynyukova, N., Hafner, A.S., Kochen, L., Sartori, F., Schuman, E.M.,  
445 and Tchumatchenko, T. (2019). How mRNA Localization and Protein Synthesis Sites  
446 Influence Dendritic Protein Distribution and Dynamics. *Neuron* *103*, 1109-1122 e1107.
- 447 24. Hafner, A.S., Donlin-Asp, P.G., Leitch, B., Herzog, E., and Schuman, E.M. (2019).  
448 Local protein synthesis is a ubiquitous feature of neuronal pre- and postsynaptic  
449 compartments. *Science* *364*.
- 450 25. Mayford, M., Baranes, D., Podsypanina, K., and Kandel, E.R. (1996). The 3'-  
451 untranslated region of CaMKII alpha is a cis-acting signal for the localization and  
452 translation of mRNA in dendrites. *Proc Natl Acad Sci U S A* *93*, 13250-13255.
- 453 26. Kuklin, E.A., Alkins, S.A., Bakthavachalu, B., Genco, M.C., Sudhakaran, I.,

- 454 VijayRaghavan, K., and Griffith, L.C. (2017). The long 3'UTR mRNA of CaMKII is  
455 essential for translation-dependent plasticity of spontaneous release in *Drosophila*  
456 *melanogaster*. *J. Neurosci. In Press*.
- 457 27. Blichenberg, A., Rehbein, M., Muller, R., Garner, C.C., Richter, D., and Kindler, S.  
458 (2001). Identification of a cis-acting dendritic targeting element in the mRNA encoding  
459 the alpha subunit of Ca<sup>2+</sup>/calmodulin-dependent protein kinase II. *Eur J Neurosci* 13,  
460 1881-1888.
- 461 28. Mori, Y., Imaizumi, K., Katayama, T., Yoneda, T., and Tohyama, M. (2000). Two cis-  
462 acting elements in the 3' untranslated region of alpha-CaMKII regulate its dendritic  
463 targeting. *Nat Neurosci* 3, 1079-1084.
- 464 29. Gao, Y., Tatavarty, V., Korza, G., Levin, M.K., and Carson, J.H. (2008). Multiplexed  
465 dendritic targeting of alpha calcium calmodulin-dependent protein kinase II,  
466 neurogranin, and activity-regulated cytoskeleton-associated protein RNAs by the A2  
467 pathway. *Mol Biol Cell* 19, 2311-2327.
- 468 30. Sudhakaran, I.P., Hillebrand, J., Dervan, A., Das, S., Holohan, E.E., Hulsmeier, J.,  
469 Sarov, M., Parker, R., VijayRaghavan, K., and Ramaswami, M. (2014). FMRP and  
470 Ataxin-2 function together in long-term olfactory habituation and neuronal translational  
471 control. *Proc Natl Acad Sci U S A* 111, E99-E108.
- 472 31. Guo, H. (2018). Specialized ribosomes and the control of translation. *Biochem Soc*  
473 *Trans* 46, 855-869.
- 474 32. Fusco, C.M., Desch, K., Dorrbaum, A.R., Wang, M., Staab, A., Chan, I.C.W., Vail, E.,  
475 Villeri, V., Langer, J.D., and Schuman, E.M. (2021). Neuronal ribosomes exhibit  
476 dynamic and context-dependent exchange of ribosomal proteins. *Nature*  
477 *communications* 12, 6127.
- 478 33. L., T., and L., L. (1999). Mosaic Analysis with a Repressible Cell Marker for Studies  
479 of Gene Function in Neuronal Morphogenesis. *Neuron* 22, 451-461.
- 480 34. Schindelin, J., Arganda-Carreras, I., Frise, E., Kaynig, V., Longair, M., Pietzsch, T.,  
481 Preibisch, S., Rueden, C., Saalfeld, S., Schmid, B., et al. (2012). Fiji: an open-source  
482 platform for biological-image analysis. *Nature methods* 9, 676-682.
- 483 35. A., S.B., L., A.H., J., R.J., WangJ., and C.-F., W. (1994). Improved stability of  
484 *Drosophila* larval neuromuscular preparations in haemolymph-like physiological  
485 solutions. *Journal of Comparative Physiology* 175, 179-191.
- 486

## 487 **METHODS DETAILS**

### 488 **Fly strains**

489 Flies (*Drosophila melanogaster*) were raised on dextrose/cornmeal/yeast food at 25°C with a  
490 12h:12h light-dark cycle. Male and female flies were collected at eclosion and aged for 2-4  
491 days before performing immunohistochemical experiments and for 7-10 days for behavior. For  
492 GCaMP experiments, only female flies (4-8 days old) were used due to the size and clarity of  
493 their brains. *UAS-mCD8::GFP* flies [33] were a gift from Dr. Liqin Luo (Stanford University),  
494 and *EYFP::CaMKII<sup>NUT</sup>* flies [12] from Dr. Sam Kunes. *VT030559-GAL4*, *A2bp1-RNAi*  
495 (110518), *Mub-RNAi* (105495), *Orb2-RNAi* (107153) and *Rbp1-RNAi* (110008) flies were  
496 obtained from VDRC Stock Center. *UAS-GFP::RPL10*, *UAS-MCP::RFP*, *UAS-GFP*,  
497 *20XUAS-GCaMP6f*, *UAS-Flp*, *Mub<sup>[MI08161]/TM3SbSer</sup>* (43942) and *CaMKII<sup>[MI03976]</sup>* (60770)  
498 flies were ordered from Bloomington *Drosophila* Stock Center. All transgenic, MiMIC  
499 conversion and CRISPR injections were performed by Rainbow Transgenics (Camarillo, CA).

500

### 501 **Creation of mMaple3-UTR and myrGFP-MS2-UTR transgenic lines**

502 For the mMaple3 lines, all 3'UTR fragments were amplified from the *Canton-S* wild type fly  
503 genome. The list of PCR primers is in Table S1. The mMaple3 plasmids were a gift of Dr.  
504 Margret Stratton (UMASS Amherst). To make the *UAS-mMaple3-long 3'UTR* line, the  
505 mMaple3 fragment and the long 3'UTR fragment were amplified and then inserted into the  
506 pUAST-attB plasmid (Addgene, 8489bp) using the Gibson assembly method. The mMaple3  
507 fragment was followed by the long 3'UTR fragment. For other 3'UTR lines, we used the same  
508 mMaple3 fragment and pUAST-attB plasmid. For the *UAS-mMaple3* control line, only the  
509 mMaple3 sequence was put into the pUAST-attB plasmid. For the *UAS-5'UTR-mMaple3* fly  
510 strain, the zygotic 5'UTR was amplified by PCR and inserted before the mMaple3 fragment.  
511 All plasmids were checked by sequencing. Plasmids were injected into *phiC31-attP* flies  
512 (Bloomington Stock Center #79604) which have attP sites on the second chromosome to allow  
513 targeted integration. The progeny of injected flies was screened by *w<sup>+</sup>* red eye marker, and then  
514 checked by PCR and sequencing.

515 Transgenic *myrGFP-MS2-UTR* lines were created by site-specific insertion of pJFRC-  
516 *myrGFP-MS2-long-3'UTR* and pJFRC-*myrGFP-MS2-short-3'UTR* plasmids into *phiC31-*  
517 *attP* docking site (Bloomington Stock Center #79604). To construct these plasmids, long or  
518 short 3'UTR sequences were amplified from *Canton-S* flies and inserted into the XbaI digested  
519 pJFRC12-10XUAS-IVS-*myrGFP* plasmid (Addgene #26222) using the Gibson assembly  
520 method. The MS2 sequence was amplified from the TRICK plasmid obtained from Dr. Jeffrey  
521 A. Chao (Friedrich Miescher Institute for Biomedical Research, Basel, Switzerland) and cloned  
522 between the GFP and the *CaMKII* UTR sequence to create pJFRC-*myrGFP-MS2-long-3'UTR*  
523 and pJFRC-*myrGFP-MS2-short-3'UTR* plasmids. The PCR primers are listed in Table S1. The  
524 injections of these plasmids were performed by the fly facility at Bangalore Life Science  
525 Cluster (BLiSC).

526

#### 527 **Creation of endogenous *CaMKII* UTR deletion fly and *CaMKII*<sup>coding-3P3-RFP</sup> fly**

528 To make the endogenous *CaMKII* UTR deletion fly (*CaMKII*<sup>Udel</sup>), we designed a guide RNA  
529 which recognize a site in the *CaMKII* 3'UTR region (Table S2). The guide RNA was cloned  
530 into pU6 plasmids (Addgene, #45946). To replace the full 3'UTR region precisely, we made a  
531 donor plasmid which contained two homology arms: the left arm was a 2 kb length fragment  
532 which preceded the stop codon TAA, and the right arm is a 2 kb-length fragment which  
533 followed the last nucleotide of the full 3'UTR. Between the two arms was an inverted-attP  
534 flanked 3xP3-RFP fragment (Addgene, #80898), which was used as a marker to check insertion  
535 (*CaMKII* Udel-homologous arms plasmid in supplemental plasmids). A mixture of guide RNA  
536 plasmid and the donor plasmid was injected into Cas9 flies (*y,sc,v; nos-Cas9/CyO; +/+*). By  
537 the same strategy, we designed two guide RNAs (Table S2) which recognize the beginning and  
538 Exon 8 of *CaMKII* coding region separately, and a donor plasmid (*CaMKII* coding-  
539 homologous arms plasmid in supplemental plasmids) to make the *CaMKII*<sup>coding-3P3-RFP</sup> fly.

540 After crossing to *ci<sup>D</sup>/ey<sup>D</sup>* flies, the F1 progeny with the RFP marker were selected as  
541 candidates. Correct integrations were confirmed by PCR and sequencing with primers which  
542 bind to outside the regions of the integrated junctions.

543

#### 544 **Creation of endogenous *CaMKII* UTR knock-in fly lines**

545 To make *CaMKII*<sup>U<sub>Long</sub></sup> flies, the long 3'UTR sequence was amplified and flanked by two  
546 inverted-attB sites, then cloned into the pBS-KS-attB2 plasmid (Addgene, #62897). This  
547 plasmid was injected into *CaMKII*<sup>U<sub>del</sub></sup> flies, with plasmids that expressed phiC31 recombinase.  
548 F1 progeny without RFP marker were selected as candidates, and further confirmation by PCR  
549 and sequencing were performed. Using the same strategy, we amplified the short 3'UTR  
550 sequence and made *CaMKII*<sup>U<sub>Short</sub></sup> flies. For the *CaMKII*<sup>Δ<sub>MubS</sub></sup> fly, we deleted 23 bp containing  
551 the two Mub binding sites from the long 3'UTR sequence. For the *CaMKII*<sup>Frt-3'UTR-Frt</sup> fly, the  
552 whole 3'UTR flanked by two Frt sites were cloned. The recombination plasmids are listed in  
553 the supplemental plasmids. All flies have been checked by PCR and sequencing with primers  
554 outside of the insertion fragment.

555

#### 556 **Creation of *Frt-stop-Frt-EGFP::CaMKII* fly line**

557 For the *Frt-stop-Frt-EGFP::CaMKII* fly line, we amplified the stop sequence which is flanked  
558 by two Frt sites, *EGFP* sequence, and *CaMKII* sequence between two attP sites of *CaMKII*<sup>coding-  
559 3P3-RFP</sup> fly. These fragments were assembled in order and cloned into the pBS-KS-attB2  
560 plasmid (*Frt-stop-Frt-EGFP-CaMKII* plasmid in supplemental plasmids). This plasmid was  
561 injected into *CaMKII*<sup>coding-3P3-RFP</sup> flies, with plasmids that expressed phiC31 recombinase. F1  
562 progeny without RFP marker were selected as candidates, and further confirmation by PCR  
563 and sequencing were performed.

564

#### 565 **Creation of endogenous *CaMKII-GAL4*, *Mub-GAL4* and *EGFP::Mub* flies**

566 To make the endogenous *CaMKII-GAL4* fly strain, the phase 1 T2A-GAL4 plasmids (Addgene,  
567 #62897) and pBS130 plasmids (Addgene, #26290) which encode phiC31 integrase were  
568 injected into *CaMKII*<sup>[M103976]</sup> flies. Progeny were crossed to *yw*, *UAS-mCD8::EGFP* flies to  
569 check for GAL4 insertion. Male flies with yellow marker were selected as candidates and  
570 checked for GFP expression to obtain the insertion lines which were in the correct orientation.

571 For *Mub-GAL4* flies, we used the same strategy, and phase 0 T2A-GAL4 plasmids (Addgene,  
572 #62896) were injected into the *Mub*<sup>[M108161]</sup>/*TM3*, *SbSer* flies.

573 For *EGFP::Mub* flies, we designed a guide RNA which recognized the beginning of *Mub*  
574 (Table S2) and a donor plasmid (*EGFP::Mub* plasmid in supplemental plasmids). The guide  
575 RNA was cloned into pU6 plasmids (Addgene, #45946) and injected into Cas9 flies with the  
576 donor plasmid. Correct integrations were confirmed by PCR and sequencing with primers  
577 which bind outside the regions of the integrated junction.

578

### 579 **Dissection and immunohistochemistry**

580 Fly brains (males and females, 2-4 days old) were dissected in cold Schneider's Insect Medium  
581 (Sigma, S0146). To minimize any systemic error caused by the order of dissection and length  
582 of freezing, all fly lines were frozen on ice at the same time. Then we dissected one fly from  
583 each line, and performed the second round dissection. After dissection the brain samples were  
584 fixed in 4% PFA solution for 45 mins at room temperature, then washed 3x30 mins in 0.5%  
585 Triton-PBS (PBST) solution. For the *mMaple3-UTR* lines, the samples were mounted anterior  
586 side up in Vectashield (Vector Labs, Burlingame, CA) mounting medium after washing. For  
587 brains that needed antibody staining, after fixation and washing, the samples were blocked in  
588 10% normal goat serum solution for 1 hour, and incubated in primary antibody solutions for 2-  
589 3 days. Primary antibody solutions were removed, and the samples were washed in PBST  
590 solution for 3x30 mins. After that the samples were incubated in secondary antibody solutions  
591 overnight. After 3x30 mins PBST washing, the same mounting protocol was performed  
592 afterwards.

593 For CaMKII staining the fixation time was shortened to 30 minutes. The primary antibodies  
594 used were: mouse anti-CaMKII (1:10,000, Cosmo CAC-TNL-001-CAM), rabbit anti-DsRed  
595 (1:150, Takara, 632496) and rabbit anti-GFP (1:1000, Thermo Fisher A-11122). DAPI was  
596 used at 1:1,000 (Invitrogen, D1306). Alexa Fluor 488 anti-mouse antibody (Invitrogen,  
597 A28175) and Alexa Fluor 635 anti-rabbit antibody (Invitrogen, A-31576) were used as  
598 secondary antibodies at 1:200 dilutions.



599

## 600 **Image processing and intensity analysis**

601 Images were taken using Leica SP5 confocal microscope under a 20x objective lens, and then  
602 analyzed using ImageJ Fuji software [34]. For comparisons between several lines, all images  
603 were taken at the same laser strengths, gains and all other settings. To quantify the intensity of  
604 axonal MB regions, we selected all consecutive slices which contain MB lobes, chose the  
605 middle slice as the representative picture and outlined all lobes as the region of interest (ROI).  
606 We quantified the mean intensity of that region to be analyzed further. To quantify the intensity  
607 of somatic regions, we checked all consecutive slices that contain the cell bodies, chose the  
608 middle slice, outlined all the cell bodies in the slice and quantified mean intensity of the  
609 outlined ROI. Further analysis of the intensity was performed using GraphPad (GraphPad  
610 Software, San Diego, CA) program.

611

## 612 **Real-time PCR experiments and quantification**

613 For each genotype, RNA was extracted from approximately 100 males and female fly heads  
614 using the Trizol Reagent (Thermo Fisher). The age of the flies was 2-4 days. RNA samples (1  
615 ug) from each genotype were reverse-transcribed using PrimeScript 1st strand cDNA Synthesis  
616 Kit (Takara). Quantitative real-time PCR experiments were performed using TB Green  
617 Advantage qPCR premixes kit (Takara) on the Thermocycler (Eppendorf Realplex2). The  
618 primers for CaMKII, mMaple3 and ribosomal gene rp49 (Table S3) were ordered from Eton  
619 company. Quantification of rp49 was used for normalization.

620

## 621 **Western Blotting and quantification**

622 Flies heads (10 flies per sample, males and females) were ground in loading buffer  
623 (NuPAGE™ LDS Sample Buffer), heated at 70°C for 10 minutes, and then 2-Mercaptoethanol  
624 was added to the samples. Proteins were separated by SDS-PAGE (NuPAGE™ Bis-Tris  
625 Protein Gels, Invitrogen), and transferred to nitrocellulose membrane (Amersham) in transfer  
626 buffer (NuPAGE). The membranes were blocked for 1 hour (blocking buffer for fluorescent

627 western blotting, Rockland Immunochemicals), and then incubated with mouse anti-CaMKII  
628 (1:400, Cosmo) and mouse anti-Actin (1:1000, Millipore) solution overnight. Secondary  
629 antibody was anti-mouse IgG DyLight™ 680 conjugated pre-adsorbed antibody (1:5000,  
630 Rockland Immunochemicals).

631 Membranes were scanned on a ChemiDoc™ Touch Imaging System with Image Lab™  
632 Touch Software (Bio-Rad), and quantified with Image Lab™ Software from Bio-Rad. Intensity  
633 of bands was measured with the Volume Tool and calculated using the background-adjusted  
634 volume. Intensity of CaMKII band was normalized to the actin signal in the same lane.

635

### 636 **Appetitive and aversive associative learning assays**

637 Appetitive and aversive associative olfactory learning experiments were performed in an  
638 environment room in red light at 25°C and 70% humidity. Age of the flies (males and females)  
639 was between 7-10 days. The two odors used were 4-methylcyclohexanol (MCH) (Sigma,  
640 153095) and 3-octanol (OCT) (Sigma, 218405) which were diluted in mineral oil at 10%  
641 concentration.

642 For the appetitive learning, filter papers were prepared with 2M sucrose, with blank filter  
643 papers used as control. Before training, the flies were starved to 10% mortality. 50-100 flies  
644 were loaded into a vial and given approximately 10 min acclimation in the apparatus. After  
645 acclimation, they were exposed to one odor (CS+) with the sucrose paper for 1 minute, and  
646 then to the other odor (CS-) with the blank paper for 1 minute with a 1-minute interval. For  
647 aversive learning, the CS+ was exposed with 60 V electric shock for 1 minute, and then CS- for  
648 1 minute with 1-minute interval.

649 After training, the flies were allowed to choose between the two odors for 2 minutes. A  
650 preference index (PI) was calculated as [(number of flies in CS+)- (number of flies in CS-)]/  
651 [(number of flies in CS+) + (number of flies in CS-)]. For each genotype, two groups of flies  
652 were trained, one with MCH as CS+ and the other with OCT as CS+. The final learning index  
653 was calculated as the average of PIs from the two reciprocal trials.

654

## 655 **Functional calcium imaging**

656 All imaging experiments were performed using a dissected brain preparation. Briefly, female,  
657 4-8 day old brains were dissected in cool HL3.1 and placed into an imaging chamber. The  
658 dissected brains were allowed to recover for about 10 mins before stimulation. An electrode  
659 was used to stimulate olfactory projection neurons by putting the end to the antennal lobe.  
660 Perfusion flow was established over the brain with a gravity-fed ValveLink perfusion system  
661 (Automate Scientific, Berkeley, CA). Imaging was performed using an Olympus BX51WI  
662 fluorescence microscope (Olympus, Center Valley, PA) under 40x water immersion lens. The  
663 calcium signals were recorded using a charge-coupled device camera (Hamamatsu ORCA  
664 C472-80-12AG).

665 Hemolymph-like saline (HL3.1) consisting of (in mM) 70 NaCl, 5 KCl, 0.1 CaCl<sub>2</sub>, 20  
666 MgCl<sub>2</sub>, 10 NaHCO<sub>3</sub>, 5 trehalose, 115 sucrose, 5 HEPES; pH 7.1-7.2 [35] was continuously  
667 perfused into the imaging chamber. Dopamine and acetylcholine were purchased from Sigma–  
668 Aldrich (St Louis, MO). For the *ex vivo* learning paradigm, the brains were first given 5  
669 stimulation trains (20 pulses at 100 Hz; pulse width is 1 millisecond, and interpulse interval is  
670 9 milliseconds) with 15 seconds intertrain interval to establish baseline. Calcium responses to  
671 the 5 trains were averaged to calculate the “Pre” responses. The brain was allowed to rest for  
672 45 seconds before induction. Pairing-dependent plasticity (PDP) [21] was induced by pairing  
673 dopamine (10 micromolar) perfusion with 12 trains of AL stimulation (5 seconds inter-train  
674 interval; the same train profile as described above). After 15 minutes we repeated the 5 trains  
675 of antennal lobe stimulations to measure the “Post” response. For acetylcholine perfusion  
676 experiments, the dissected brains were exposed to 4 mM or 10 mM acetylcholine for 1 min,  
677 and then washed with HL3.1 saline.

678 The alpha prime tips ( $\alpha'$ ) of the MBs were selected as regions of interest. Signals were  
679 analyzed using custom software developed in ImageJ (National Institute of Health, Bethesda,  
680 MD). The percent change of fluorescence was calculated as  $\Delta F/F = (F_n - F_0)/F_0 \times 100\%$ , where  
681  $F_n$  is the fluorescence at time point  $n$ , and  $F_0$  is the fluorescence at time 0. The averages of  
682 maximum percent change were determined as the response value for each trial.

683 Statistical analyses were performed using Matlab (The MathWorks). For PDP, a paired t-  
684 test was used to determine statistical significance between pre and post responses. For  
685 acetylcholine response, one-way ANOVA followed by Bonferroni post-hoc test was used to  
686 determine the significance among groups.

687

### 688 **Statistics**

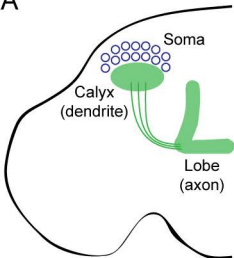
689 We used GraphPad (GraphPad Software, San Diego, CA) to make histograms and analyze data  
690 except as noted. For comparison among three or more groups, we performed one-way ANOVA,  
691 and followed with Bonferroni post-hoc test to compare difference between groups. For  
692 comparison between two groups, we used the Student T-test.  $P < 0.05$  is indicated as \*,  $p < 0.01$   
693 is indicated as \*\*, and  $p < 0.001$  is indicated as \*\*\*.

694

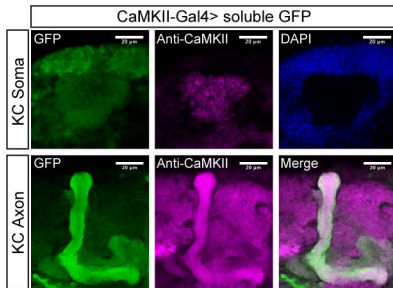
### 695 **Data availability**

696 The data generated and analyzed during this study are available from the corresponding  
697 author on request.

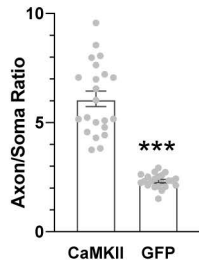
A



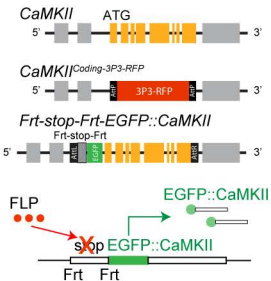
B



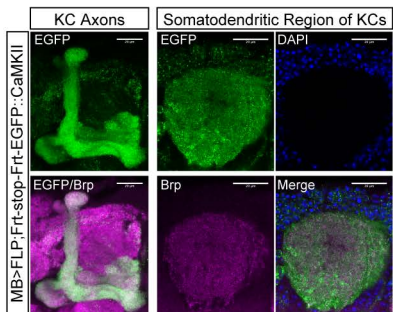
C



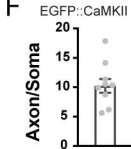
D



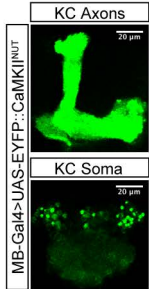
E



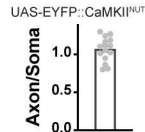
F

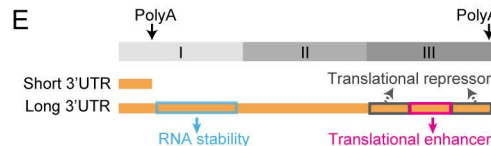
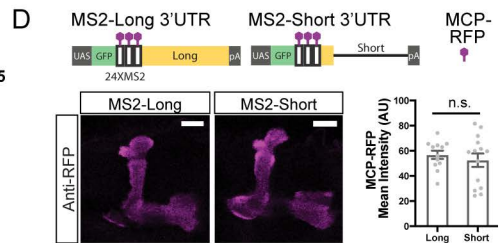
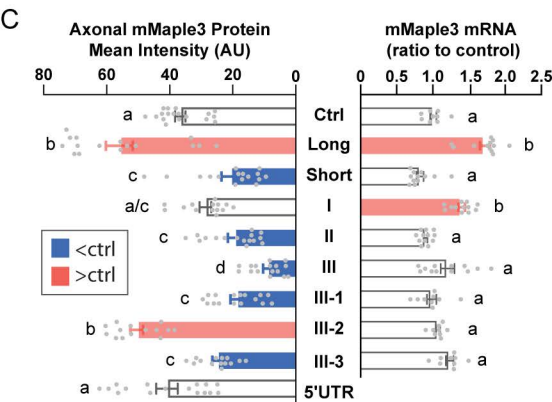
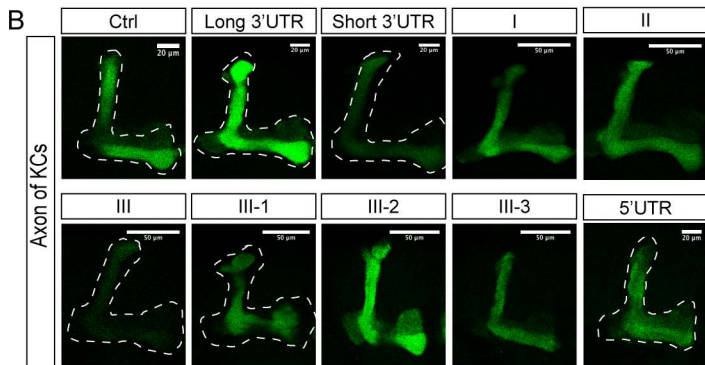
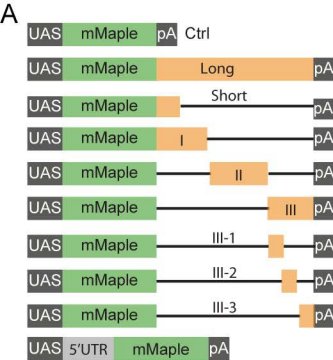


G

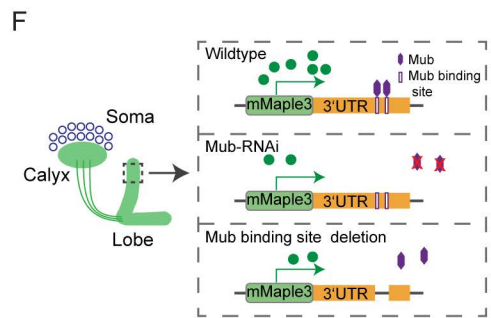
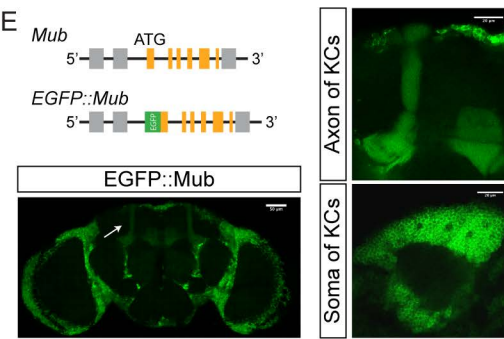
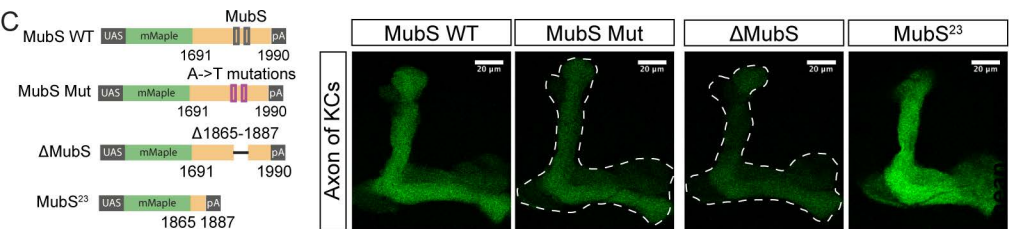
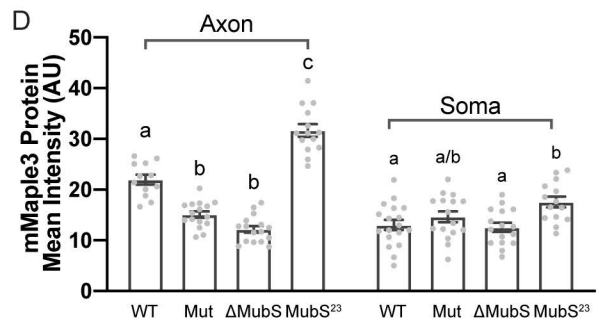
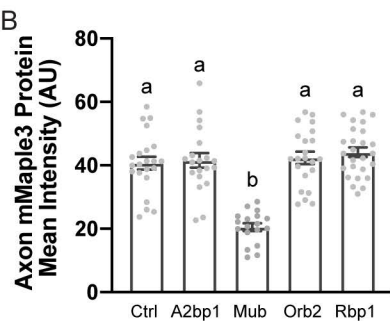
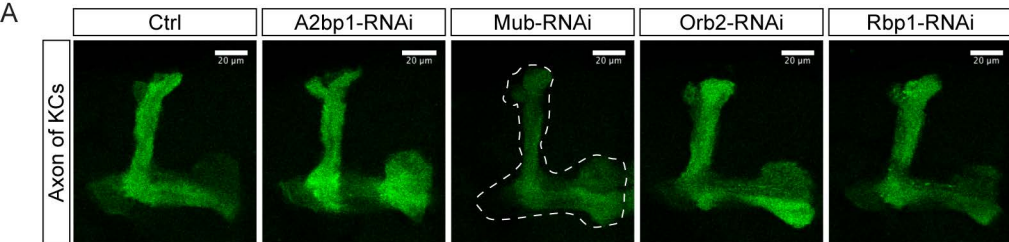


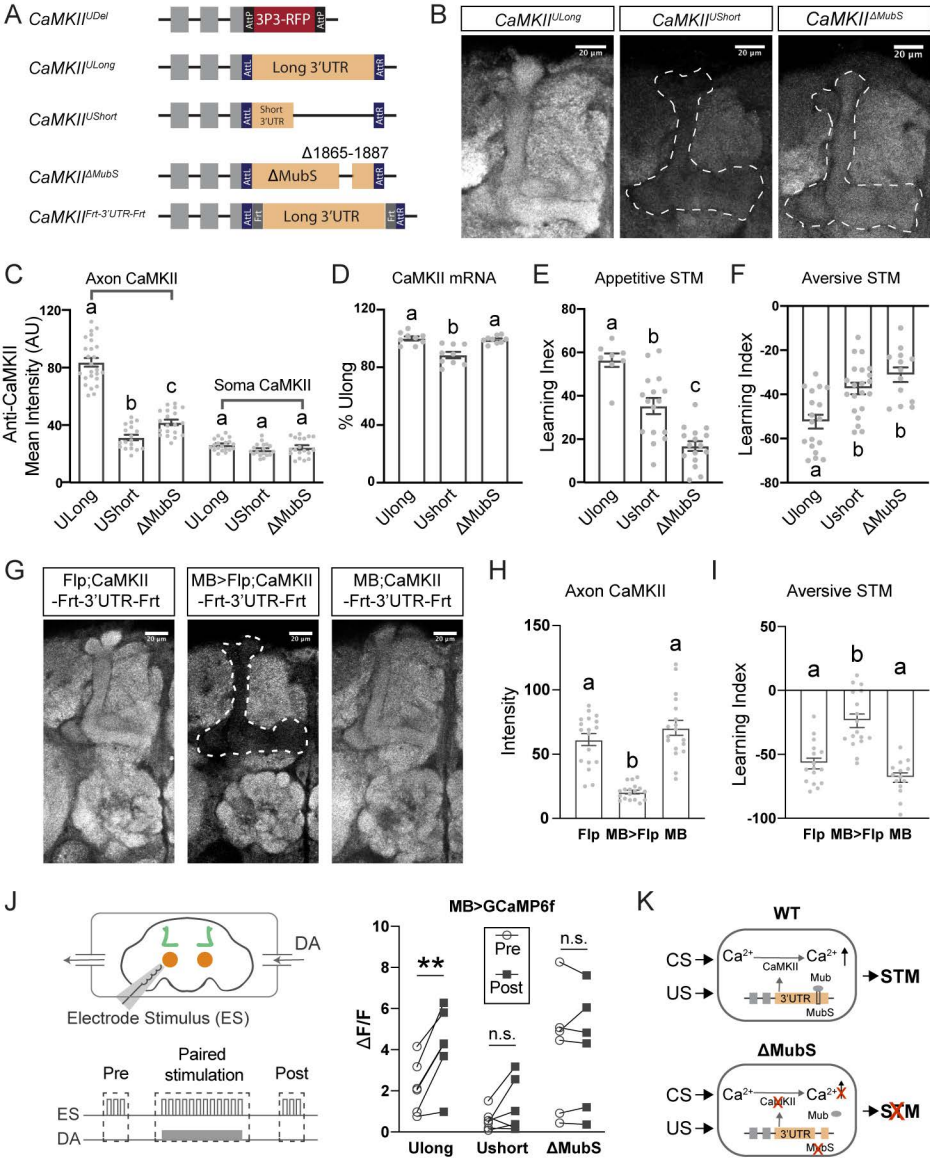
H











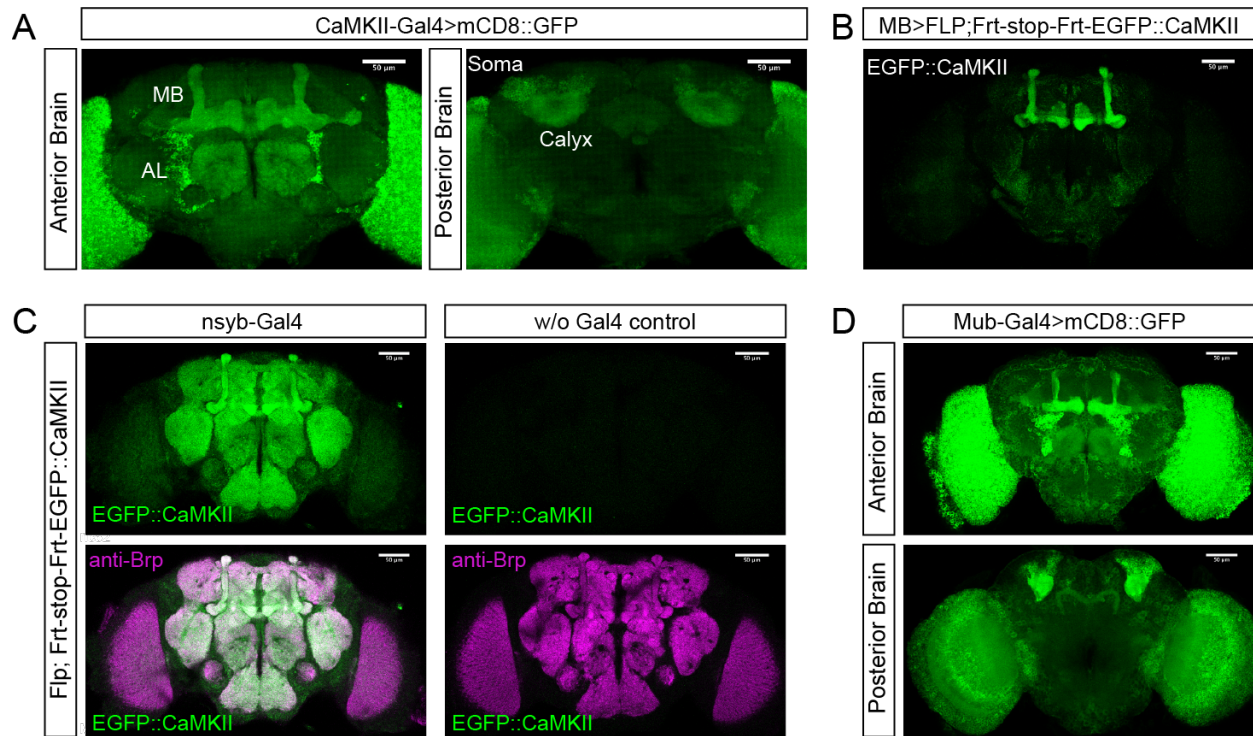


**Figure S1. *CaMKII* and *Mub* genetic reagents, related to Figures 1 and 3**

(A) The MiMIC transgene *Mi{MIC} CaMKII<sup>M103976</sup>*, which is located in the ninth intron of the *CaMKII* gene was converted to a GAL4 line using standard techniques [33]. Confocal stacks of the anterior brain (left) and the posterior brain (right) from *CaMKII>mCD8::GFP* animals expressing membrane-bound GFP. (B) EGFP::CaMKII protein expression exclusively in Kenyon cells using *VT030559-GAL4* (denoted in this paper as “MB-GAL4”) to drive the FLP recombinase to remove stop sequences. (C) EGFP::CaMKII expression using pan-neuronal GAL4 to drive FLP. Left; *nsyb-GAL4* pan-neuronal flip out. Right; no EGFP signal is seen when no GAL4 is present. (D) The MiMIC transgene *Mi{MIC}mub<sup>M108161</sup>*, which is located in the first intron of the *mub* gene, was converted to a GAL4 line using standard techniques. Confocal stacks of the anterior brain (top) and the posterior brain (bottom) from *mub>mCD8::GFP* animals expressing membrane-bound GFP show cells which transcribe *mub*. Scale bars = 50  $\mu$ m for each panel.

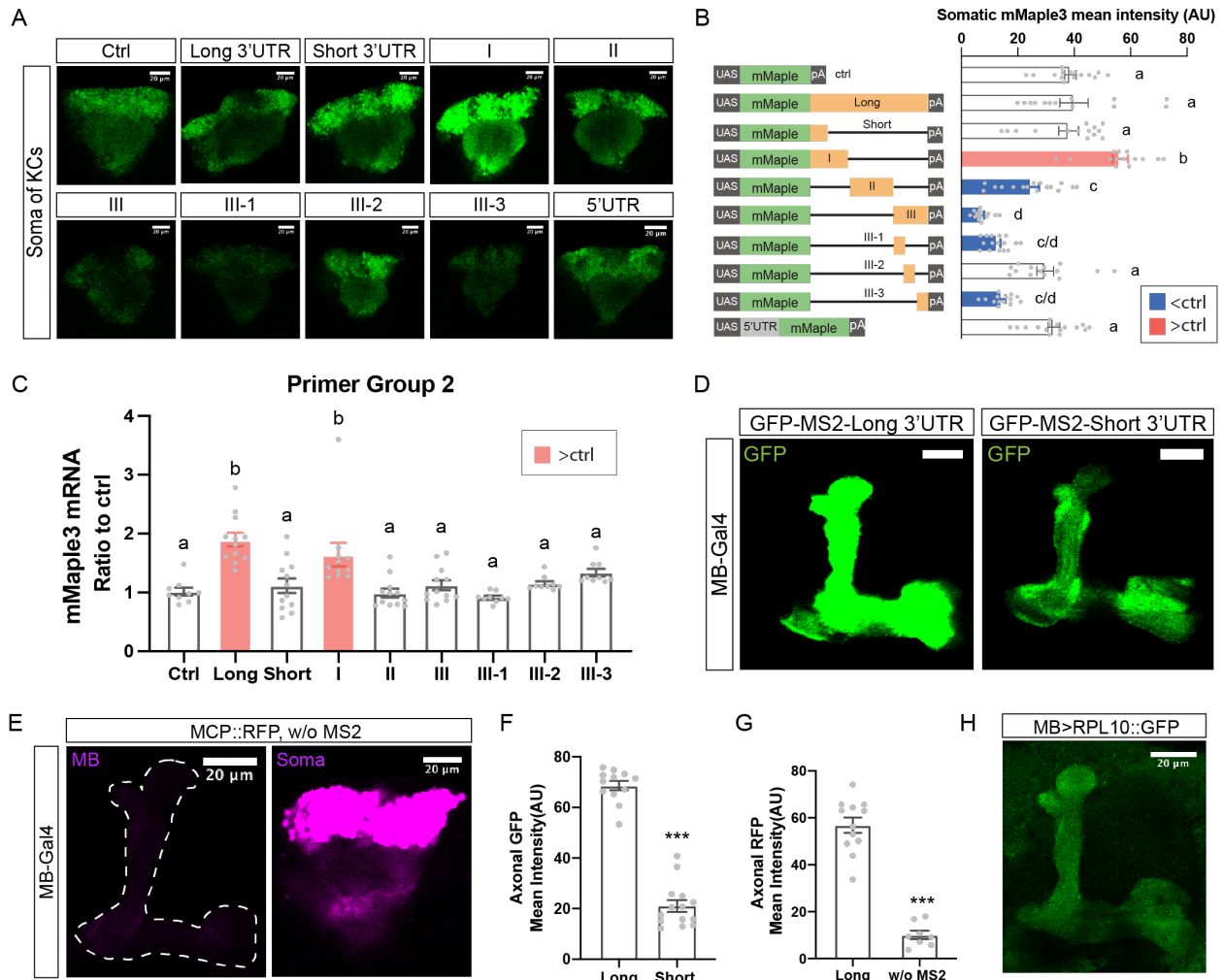


**Figure S2. Cis-elements in the *CaMKII* 3'UTR which support axonal protein synthesis in MB, related to Figure 2**

(A) Representative images of MB somatic mMaple3 protein expression from *MB>mMaple3* brains. Scale bars = 20  $\mu$ m. (B) Left, cartoon of transgenes. Right, quantification of somatic mMaple levels and comparison to control transgene. N = 14-18. (C) qPCR of mRNA from adult *MB>mMaple3* heads using a second, independent primer set against mMaple3. N = 9-12. These data confirm that the proximal 3'UTR-I contains an mRNA stability element. For both panels B and C, red bars indicate significant increase relative to control, blue indicates decrease. (D) Representative images of the MB axonal region from *MB>24XMS2-myrGFP-UTR* animals. Left panel shows myrGFP protein reporter with long 3'UTR and right panel shows short 3'UTR. (E) Axonal MCP::RFP accumulation requires the expression of the MS2 transgene. Left panel shows MB axonal region from *MB>RFP::MCP-nls* animals that are not expressing an MS2-containing

transgene. Right panel shows that all of the RFP::MCP-nls protein is sequestered in nuclei. (F) Quantification of myrGFP protein levels from panel D. N = 12-14. (G) Axonal RFP levels in animals with no MS2 transgene compared to animals co-expressing the *UAS-24XMS2-myrGFP* transgene. N = 8-12. (H) Ribosomes are present in the MB axonal compartment. Image shows MB region from *MB>RPL10::GFP* adult brain. This GFP-tagged ribosomal protein has been shown to co-assemble with endogenous ribosomes [15]. Data are shown as mean  $\pm$  SEM and quantified by one-way ANOVA with Bonferroni post-hoc test or Student's t-test accordingly. Statistical differences are indicated by letters in panels B and C; groups that are not significantly different have the same letter. \*\*\* indicates that  $P < 0.001$  in panels F and G. Gray dots show individual values. Scale bars = 20  $\mu$ m for each panel.

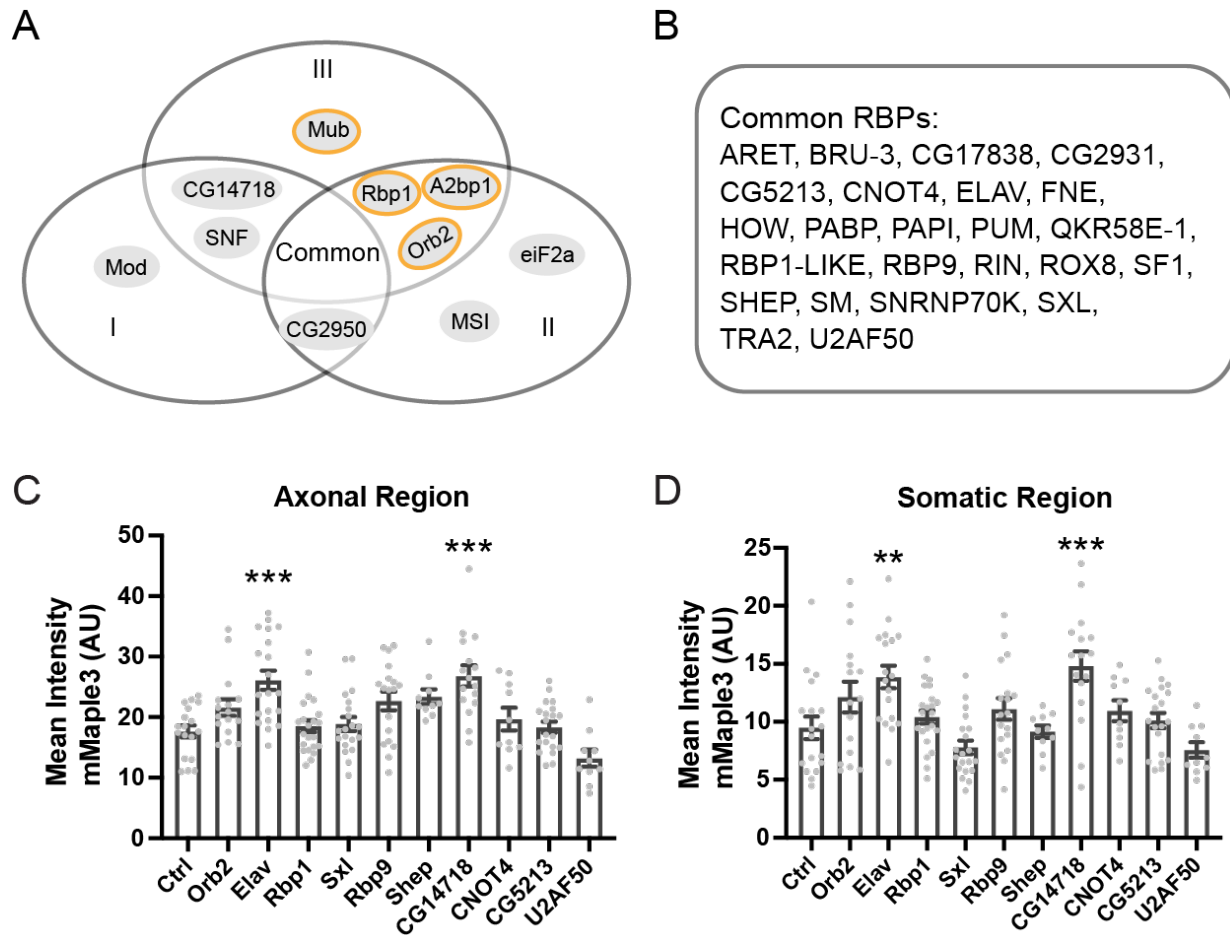


**Figure S3. *In silico* predictions of RNA-binding protein and candidate *trans*-acting repressors, related to Figure 3**

(A) The 3'UTR of the *CaMKII* gene was run through RBPmap [17] at medium stringency to obtain a list of potential RBP binding sites for screening. (B) Common RBPs found in all three fragments. (C/D) Candidate RBPs for screening were selected from the RBPmap list using the criteria that they must have at least one site in Fragment III and be predicted with  $P < E-04$ . RNAis for candidate RBP regulators were co-expressed in MB with *UAS-mMaple3-III*. Quantification of mMaple3 protein in *MB>mMaple3-III* ± RNAi brains shows that knocking down *elav* or *CG14718* significantly increased mMaple3 levels in both somatic and MB axonal regions. Data are shown as mean ± SEM and quantified by one-way ANOVA with Bonferroni post-hoc test.  $N = 10-22$  for both panels. \*\*  $P < 0.01$ ; \*\*\*  $P < 0.001$ . Gray dots show individual values.



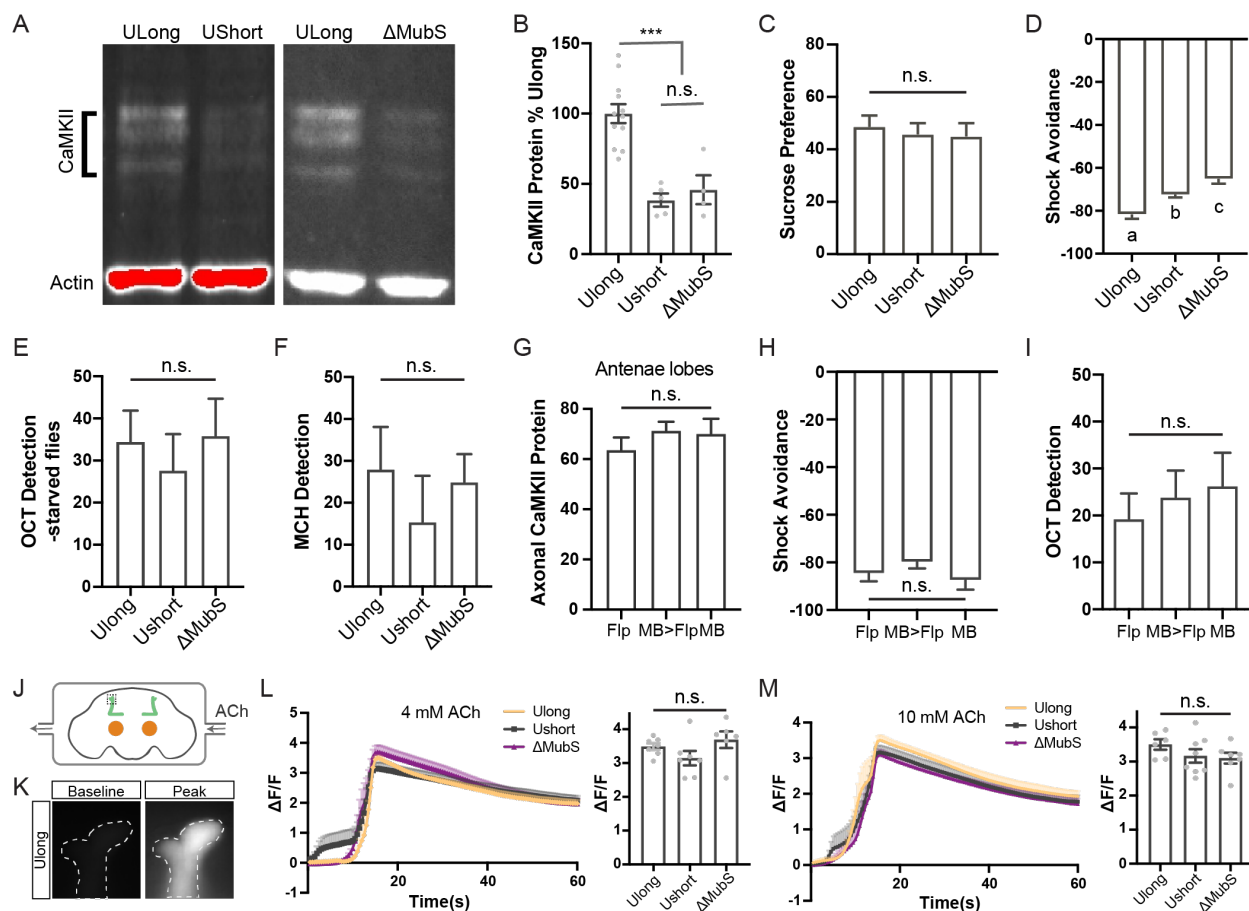


**Figure S4. Loss of *CaMKII* 3'UTR reduces CaMKII protein but leaves odor and sucrose response unaffected, related to Figure 4**

(A) Representative immunoblots with anti-CaMKII and anti-actin for normalization. SDS-PAGE for immunoblotting with monoclonal anti-CaMKII antibody showed that both *CaMKII*<sup>UShort</sup> and *CaMKII*<sup>ΔMubS</sup> have reduced total-head CaMKII compared to *CaMKII*<sup>ULong</sup> which has the WT full length 3'UTR. (B) Quantification of CaMKII protein normalized to actin. N = 4-12. (C) *CaMKII*<sup>UShort</sup> and *CaMKII*<sup>ΔMubS</sup> show similar sucrose preference to *CaMKII*<sup>ULong</sup>. N = 6-9. (D) *CaMKII*<sup>UShort</sup> and *CaMKII*<sup>ΔMubS</sup> show similar shock avoidance to *CaMKII*<sup>ULong</sup>. N = 8 for each group. (E) *CaMKII*<sup>UShort</sup>, *CaMKII*<sup>ΔMubS</sup> and *CaMKII*<sup>ULong</sup> show similar ability to detect octanol, even when starved N = 10-16. (F) *CaMKII*<sup>UShort</sup>, *CaMKII*<sup>ΔMubS</sup> and *CaMKII*<sup>ULong</sup> show similar ability to detect MCH, N = 8. (G) Quantification of CaMKII in antennae lobes showed that CaMKII protein level was unaffected when 3'UTR was specifically knocked out in MB. N = 16 for each group. (H) MB-specific knockout of *CaMKII* 3'UTR sequences didn't affect shock



avoidance. N = 8-12. (I) MB-specific knockout of *CaMKII* 3'UTR sequences didn't affect octanol detection. N = 10-26. (J) Diagram of ACh perfusion setup. Different concentrations ACh were perfused across the imaging region. The dashed square shows the recording area, the  $\alpha/\alpha'$  tip region. (K) Representative pictures of the recording area for baseline and peak calcium responses of *U*Long flies (*MB/20xGCaMP6f; CaMKII<sup>U</sup>Long*). (L) With 4 mM ACh perfusion, *CaMKII<sup>U</sup>Short* and *CaMKII<sup>ΔMubS</sup>* flies showed comparable calcium responses to *CaMKII<sup>U</sup>Long*. N = 6-7. (M) With 10 mM ACh perfusion, calcium responses of *CaMKII<sup>U</sup>Short* and *CaMKII<sup>ΔMubS</sup>* were also similar to that of *CaMKII<sup>U</sup>Long*. N = 6-8. The genotypes in panels L and M are: *MB/20xGCaMP6f; CaMKII<sup>U</sup>Long*, *MB/20xGCaMP6f; CaMKII<sup>U</sup>Short* and *MB/20xGCaMP6f; CaMKII<sup>ΔMubS</sup>*. Data are shown as mean  $\pm$  SEM and quantified by one-way ANOVA with Bonferroni post-hoc test. \*\*\* P < 0.001, and n.s. indicates no significant difference. Statistical differences in panel D are indicated by letters; groups that are significantly different have different letter.

**Table S1. Primer list for transgenic flies.**

Fly strain	Primer name	Primer sequence
UAS-mMaple3	mMaple3 F	TAACAGATCTGCGGCCGCGGCTCGAGA TGGTGAGCAAAGGCGAGGA
	mMaple3 R	AGGTTCCCTTCACAAAGATCCTCTAGAT TACTTGTAGAGTTCGTCCATGCTGT
UAS-5'utr-mMaple3	mMaple3 F	TTCTTAAGTGTGCCATCGCGATGGTGA GCAAAGGCGAGGA
	mMaple3 R	AGGTTCCCTTCACAAAGATCCTCTAGAT TACTTGTAGAGTTCGTCCATGCTGT
	5'UTR F	TAACAGATCTGCGGCCGCGGCTCGAG AGTCAGTATTGAATTCGATTTTCA
	5'UTR R	TCCTCGCCTTTGCTCACCATCGCGATGG CACACTTAAGAA
UAS-mMaple3-long	mMaple3 F	TAACAGATCTGCGGCCGCGGCTCGAGA TGGTGAGCAAAGGCGAGGA
	mMaple3 R	ATTCCATTGATTAATGCCACTTACTTGT AGAGTTCGTCCATGCTGT
	3'UTR F	ACAGCATGGACGAACTCTACAAGTAAT GGGCATTAATCAATGGAAT
	3'UTR R	AGGTTCCCTTCACAAAGATCCTCTAGAA AAATTGCATTATGCTTTGA
UAS-mMaple3-short	mMaple3 F	TAACAGATCTGCGGCCGCGGCTCGAGA TGGTGAGCAAAGGCGAGGA
	mMaple3 R	ATTCCATTGATTAATGCCACTTACTTGT AGAGTTCGTCCATGCTGT
	3'UTR F	ACAGCATGGACGAACTCTACAAGTAAT GGGCATTAATCAATGGAAT
	3'UTR R	AGGTTCCCTTCACAAAGATCCTCTAGAA AATTAATAAAATTTGCACT
UAS-mMaple3-I	mMaple3 F	TAACAGATCTGCGGCCGCGGCTCGAGA TGGTGAGCAAAGGCGAGGA
	mMaple3 R	ATTCCATTGATTAATGCCACTTACTTGT AGAGTTCGTCCATGCTGT
	3'UTR F	ACAGCATGGACGAACTCTACAAGTAAT GGGCATTAATCAATGGAAT
	3'UTR R	AGGTTCCCTTCACAAAGATCCTCTAGAG CATAATTTCAATTATTGGG
UAS-mMaple3-II	mMaple3 F	TAACAGATCTGCGGCCGCGGCTCGAGA TGGTGAGCAAAGGCGAGGA

	mMaple3 R	ATAAGTAATTCGAAGTAGTCTTACTTG TAGAGTTCGTCCATGCTGT
	3'UTR F	ACAGCATGGACGAACTCTACAAGTAAG ACTACTTCGAATTACTTAT
	3'UTR R	AGG TTCCTTCACAAAGATCCTCTAGAA TTGTTTAAATTAGCTATTT
UAS-mMaple3-III	mMaple3 F	TAACAGATCTGCGGCCGCGGCTCGAGA TGGTGAGCAAAGGCGAGGA
	mMaple3 R	TGTTATGTTTATCATATCGCTTACTTGT AGAGTTCGTCCATGCTGT
	3'UTR F	ACAGCATGGACGAACTCTACAAGTAAG CGATATGATAAACATAACA
	3'UTR R	AGG TTCCTTCACAAAGATCCTCTAGAA AAATTGCATTATGCTTTGA
UAS-mMaple3-III-1	mMaple3 F	TAACAGATCTGCGGCCGCGGCTCGAGA TGGTGAGCAAAGGCGAGGA
	mMaple3 R	TGTTATGTTTATCATATCGCTTACTTGT AGAGTTCGTCCATGCTGT
	3'UTR F	ACAGCATGGACGAACTCTACAAGTAAG CGATATGATAAACATAACA
	3'UTR R	AGG TTCCTTCACAAAGATCCTCTAGAC TGGCAAAC TTTTAAATGTG
UAS-mMaple3-III-2	mMaple3 F	TAACAGATCTGCGGCCGCGGCTCGAGA TGGTGAGCAAAGGCGAGGA
	mMaple3 R	CTTTTTACTTTAAATATATTTACTTG TAGAGTTCGTCCATGCTGT
	3'UTR F	ACAGCATGGACGAACTCTACAAGTAAA TATATTTTAAAGTAAAAAAG
	3'UTR R	AGG TTCCTTCACAAAGATCCTCTAGAG GCTTTTACCTTAGGAGCGA
UAS-mMaple3-III-3	mMaple3 F	TAACAGATCTGCGGCCGCGGCTCGAGA TGGTGAGCAAAGGCGAGGA
	mMaple3 R	TTTTCGGTTATTATTTTATATTTACTTGT AGAGTTCGTCCATGCTGT
	3'UTR F	ACAGCATGGACGAACTCTACAAGTAAT ATAAAATAATAACCGAAA
	3'UTR R	AGG TTCCTTCACAAAGATCCTCTAGAA AAATTGCATTATGCTTTGA
UAS-mMaple3-MubS WT	mMaple3 F	TAACAGATCTGCGGCCGCGGCTCGAGA TGGTGAGCAAAGGCGAGGA

	mMaple3 R	ACAAAAAGAATCAAGTACTCTTACTTG TAGAGTTCGTCCATGCTGT
	3'UTR F	ACAGCATGGACGAACTCTACAAGTAAG AGTACTTGATTCTTTTTGT
	3'UTR R	AGGTTCTTCACAAAGATCCTCTAGAA AAATTGCATTATGCTTTGA
UAS-mMaple3-MubS Mut	mMaple3 F	TAACAGATCTGCGGCCGCGGCTCGAGA TGGTGAGCAAAGGCGAGGA
	mMaple3 R	ACAAAAAGAATCAAGTACTCTTACTTG TAGAGTTCGTCCATGCTGT
	3'UTR Fragment 1 F	ACAGCATGGACGAACTCTACAAGTAAG AGTACTTGATTCTTTTTGT
	3'UTR Fragment 1 R	TTCGGTAATTATTTTATAGGCTATTACC TTAGGAGCGAAAGCT
	3'UTR Fragment 2 F	TAGCCTATAAAATAATTACCGAAAATA ATTTATGTTT
	3'UTR Fragment 2 R	AGGTTCTTCACAAAGATCCTCTAGAA AAATTGCATTATGCTTTGA
UAS-mMaple3-ΔMubS	mMaple3 F	TAACAGATCTGCGGCCGCGGCTCGAGA TGGTGAGCAAAGGCGAGGA
	mMaple3 R	ACAAAAAGAATCAAGTACTCTTACTTG TAGAGTTCGTCCATGCTGT
	3'UTR Fragment 1 F	ACAGCATGGACGAACTCTACAAGTAAG AGTACTTGATTCTTTTTGT
	3'UTR Fragment 1 R	TTTGAGAAACATAAATTATTTTACCTTA GGAGCGAAAGCT
	3'UTR Fragment 2 F	AGCTTTCGCTCCTAAGGTAAAATAATT TATGTTTCTCAA
	3'UTR Fragment 2 R	AGGTTCTTCACAAAGATCCTCTAGAA AAATTGCATTATGCTTTGA
UAS-mMaple3-Mub <sup>23</sup>	mMaple3 F	TAACAGATCTGCGGCCGCGGCTCGAGA TGGTGAGCAAAGGCGAGGA
	mMaple3 R	AGGTTCTTCACAAAGATCCTCTAGAT TCGGTTATTATTTTATAGGCTTTTACTT GTAGAGTTCGTCCAT
myrGFP-MS2-long	3'UTR F	TGGGCATTAATCAATGGAATATAAACT G
	3'UTR R	GCACGCGATCAGGGGAATTG
myrGFP-MS2-short	3'UTR F	TGGGCATTAATCAATGGAATATAAACT G
	3'UTR R	AAATTAATAAAATTTGCACTAGCATCT TTATTCGCAAT

**Table S2. Guide RNA list for CRISPR/CAS9 flies.**

Fly strain	gRNA
<i>CaMKII<sup>Udel</sup></i>	GAACCCTTGAGTTATCTACT
<i>CaMKII<sup>coding-3P3-RFP</sup></i>	GGTTTCTTGCGATGCACAA
	GTTACAGCAACGCGAACGTG
<i>EGFP-Mub</i>	CGGTGCGTCCATCAAACACG

**Table S3. Primer list for qPCR experiments.**

Experiments	Primers Group	Primer sequence	
mMaple3 qPCR	Primers Group 1	Forward	CGACCTGGAGGTTAAGGAAG
		Reverse	GAAGCTCTGCTTGAAGTAGTCC
	Primers Group 2	Forward	CTACAAAGTTAAGCAAAAGGCAG
		Reverse	GTTATAGTCCTTGTCGTGGCTC
CaMKII qPCR	Primers Group	Forward	GTAACCGGTGGTGAACCTTTTGG
		Reverse	TGATTGACCGATTCCAATATTTG
Rp49 qPCR	Primers Group	Forward	AGGGTATCGACAACAGAGTG
		Reverse	CACCAGGAACTTCTTGAATC